The magnetic properties of Fe_3O_4/nonmagnetic metal/Fe hybrid systems

K. Omori, T. Kawai, N. Takahashi, T. Yanase, T. Shimada, and T. Nagahama

Citation: Appl. Phys. Lett. **110**, 212402 (2017); doi: 10.1063/1.4983700
View online: http://dx.doi.org/10.1063/1.4983700
View Table of Contents: http://aip.scitation.org/toc/apl/110/21
Published by the American Institute of Physics

The magnetic properties of Fe_3O_4/nonmagnetic metal/Fe hybrid systems

K. Omori,[1] T. Kawai,[1] N. Takahashi,[1] T. Yanase,[2] T. Shimada,[2] and T. Nagahama[2]
[1]*Graduate School of Chemical Sciences and Engineering, Hokkaido University, Kita13 Nishi8, Kita-ku, Sapporo 060-8628, Japan*
[2]*Graduate School of Engineering, Hokkaido University, Kita13 Nishi8, Kita-ku, Sapporo 060-8628, Japan*

(Received 27 February 2017; accepted 5 May 2017; published online 22 May 2017)

Fe_3O_4 possesses unique properties such as high Curie temperature and half-metallic nature and therefore can function as a high-spin-polarized electrode in spintronic devices. In order to use this compound in such devices, the magnetic characteristics of multilayers used in these devices, which include Fe_3O_4, should be highly controllable. In this study, we fabricated Fe_3O_4/Pt or Cr (0–10 nm)/Fe systems through epitaxial growth on MgO(110) substrates in order to investigate the magnetic coupling in Fe_3O_4 and metallic hybrid systems. We found that these two systems show a marked difference in the dependence of the coercive field (H_c) of the Fe layer on the nonmagnetic-metal-layer thickness. H_c for the system with Pt showed variation characteristics of interlayer exchange coupling in metal systems, while H_c increased monotonically with the thickness of the Cr layer. *Published by AIP Publishing.* [http://dx.doi.org/10.1063/1.4983700]

Spintronics, a technology that utilizes the spin degree of freedom of electrons, has been attracting much attention because of its use in devices such as spin transfer torque – random access memory (STT-RAM) and spin torque oscillators. The discovery of more phenomena related to spin current allows the development of spintronic devices, and such phenomena enable the basic technology that can be used to fabricate highly functional devices. In these phenomena, which include YIG in the spin Seebeck effect,[1] the thermal generation of spin current involving $CoFe_2O_4$[2] and the spin Hall magnetoresistance effect,[3] magnetic oxides play important roles. Therefore, the development of magnetic oxide thin films is needed in order to realize spintronic devices.

Spinel ferrites have been developed for use as electrodes in magnetic tunnel junctions (MTJs)[4,5] and as tunnel barriers in spin filter junctions.[6–8] Fe_3O_4, which is a ferromagnetic conductor, is the typical spinel ferrite so that a large number of research studies on Fe_3O_4 films have been reported so far.[9,10] In particular, the metal-insulator transition at 120 K, which is called Verwey transition,[11] has been still a matter of argument.[12–14] Furthermore, the band calculations for this material predict that it is half-metallic, and therefore, researchers are seeking the way to use Fe_3O_4 as high-spin polarized electrodes in an MTJ.[15] On the other hand, $CoFe_2O_4$, which is a ferromagnetic insulator, can behave as a spin filter tunnel barrier.[6–8] Its lattice constants (0.84 nm) easily allow epitaxial growth on MgO or Fe, being twice as large as that of MgO; therefore, the films can be integrated with Fe/MgO/Fe MTJs.[16,17] The high Curie temperature of spinel ferrites enables their use in operations at room temperature (RT). Other oxides such as perovskite have also been intensively studied for their potential use as spintronic materials[18] even though their Curie temperatures are lower than RT.

In order to use oxides in spintronic devices, magnetic properties such as the coercive field (H_c) and the shape of the hysteresis loop must be highly controlled. In such metallic systems, magnetic properties are controlled by magnetic exchange coupling. Direct exchange coupling between a ferromagnetic metal and an antiferromagnetic metal is widely used in spin valve systems.[19] Interlayer exchange coupling (IEC) is also extensively used in synthetic antiferromagnetic structures such as Co/Ru/Co systems.[20] Few works, however, have examined multilayer systems involving oxides. The Fe_3O_4(001)/Fe(001) epitaxial bilayer has been reported to exhibit antiferromagnetic coupling,[21] while the Fe_3O_4/MgO/Fe and γ-Fe_2O_3/MgO/Fe systems have been found to exhibit other types of coupling.[22] The magnetic coupling in the Fe_3O_4/MgO/Fe_3O_4 system has also been previously investigated.[23,24] Analogous to the metallic multilayer systems, hybrid multilayer systems having both a magnetic oxide and a nonmagnetic metal (NM) layer show various types of magnetic coupling.

In the present study, Fe_3O_4/Cr/Fe and Fe_3O_4/Pt/Fe hybrid systems were fabricated, and the magnetic characteristics of these systems were investigated. Since Fe/Cr/Fe is the typical system that exhibits the interlayer exchange coupling (IEC),[25] the magnetic coupling in the Fe_3O_4/Cr/Fe system was a very interesting issue. For Fe_3O_4/Pt/Fe, we chose Pt as a non-magnetic layer because Fe/Pt/Fe was also reported[26] to show IEC and Pt is hardly oxidized. If the IEC exists in the hybrid systems, the magnetic coupling would be expected to oscillate as a function of the NM layer thickness. On the other hand, the nonexistence of IEC would result in that the hysteresis loops were independent of the NM layer thickness. In this study, we found that the two systems exhibit completely different behaviors from observations on the magnetic coupling between the Fe_3O_4 and Fe layers.

We used Fe_3O_4 as a magnetic oxide layer because it is a highly spin polarized material,[15] and reports confirm its epitaxial growth on MgO substrates.[27] Samples were grown on MgO(110) substrates by using the reactive molecular beam epitaxy (MBE) method using oxygen to form MgO(110)/NiO(5 nm)/Fe_3O_4(60 nm)/Pt (t_{Pt} of 0–10 nm)/Fe(5 nm)/Al_2O_3(2 nm) and MgO(110)/NiO/Fe_3O_4/Cr(t_{Cr} of 0–10 nm)/Fe/Al_2O_3 film structures. The base pressure of the MBE chamber was 7×10^{-8} Pa. Before deposition, MgO(110)

single-crystal substrates were prebaked at 800 °C for 30 min. A NiO layer was inserted to prevent the diffusion of Mg from the MgO substrate into the Fe_3O_4 layer.[28] The Fe_3O_4(110) layer was deposited on MgO(110) by using an Fe source at 300 °C in an oxygen atmosphere at 1×10^{-4} Pa. Next, the NM layer (Pt or Cr) was grown at 130 °C in the form of a wedge (0–10 nm) by using a linear shutter. The Fe and Al_2O_3 layers were then deposited onto the NM layer at RT. The epitaxial growth and surface morphology were confirmed by reflection high-energy electron diffraction (RHEED) and atomic force microscopy, respectively. The crystal structures were investigated by X-ray diffraction (XRD) measurements. The magnetization process was monitored from the longitudinal magneto-optical Kerr effect (MOKE) at RT at a wavelength of 650 nm.

Figure 1 shows the result of the RHEED and XRD measurements for the Fe_3O_4/Pt/Fe multilayers. Figures 1(a)–1(c) show the RHEED patterns of the Fe_3O_4, Pt, and Fe layers, respectively. The electron beam was incident along the MgO[100] direction. Spotty patterns [Figs. 1(a)–1(c)] indicate that the Fe_3O_4(110) and Pt layers grew epitaxially, although their surfaces were rough. According to the XRD profile at θ–2θ, Fe_3O_4 and Pt grew in the (110) direction. Since both the NiO and Fe layers were thin, the peaks for NiO and Fe were absent, although a small peak corresponding to Fe(211) appeared at $2\theta = 82°$. The lattice parameters of MgO, NiO, Fe_3O_4, and Pt are 0.421 nm, 0.418 nm, 0.8397 nm, and 0.392 nm, respectively;[29] the lattice mismatch values for MgO/NiO, NiO/Fe_3O_4, and Fe_3O_4/Pt are −0.713%, 0.443%, and 6.63%, respectively.

The RHEED and XRD results for Fe_3O_4/Cr/Fe are shown in Fig. 2. Figures 2(a)–2(c) display the RHEED patterns of Fe_3O_4, Cr, and Fe, respectively. The surfaces of the Cr and Fe layers were rougher than those of the Fe_3O_4/Pt/Fe layer because their RHEED patterns were spottier than those of the sample with Pt. Fe_3O_4(110) peaks along with a Fe and a Cr(211) peak in the XRD profile indicate that Cr(211) grew on Fe_3O_4(110). The epitaxial growth of Cr(211) on MgO(110) is a well-known phenomenon.[30,31] Moreover, the lattice parameter of Fe_3O_4 is twice that of MgO. Therefore, it is likely that Cr(211) grew on Fe_3O_4(110) epitaxially.

In order to investigate the magnetic properties of these materials, longitudinal MOKE was used to obtain the hysteresis loops of the Fe_3O_4(110)/[Pt(t_{Pt}) or the Cr(t_{Cr})]/Fe(5 nm) system at RT. The wedge shape of the Pt or Cr layers enables the measurement of hysteresis at various Pt or Cr thicknesses in a substrate. The spot size of the MOKE was 0.1 mm, and the t_{Pt} and t_{Cr} values changed from 0 to 10 nm within 20 mm. The shapes of the hysteresis curves depended on the direction of the magnetic field (H). As shown in Fig. 3, the hysteresis curves when H was parallel to the MgO[-111] direction suggest a two-step magnetization process, while a single-step magnetization process was apparent when H was in the MgO[100] direction. In the two-step process, the abrupt magnetization switching of Fe and Fe_3O_4 occurred separately; a small switching field corresponds to the H_c value of Fe, and a large one corresponds to the H_c value of Fe_3O_4. In contrast, the magnetization switching of Fe_3O_4 progressed gradually because of crystal magnetic anisotropy when H was applied in the [100] direction; consequently, only the switching of the Fe layer was observed. Such magnetization switching was also observed by VSM measurements (not shown). The variation of the hysteresis depending on the H directions could be attributed to the crystal magnetic anisotropy of Fe_3O_4 and the anisotropic surface lattice of the MgO(110) substrates.[5]

In Fig. 4(a), the hysteresis curves for various t_{Pt} are shown. At a t_{Pt} value of 0, the H_c value of Fe was much

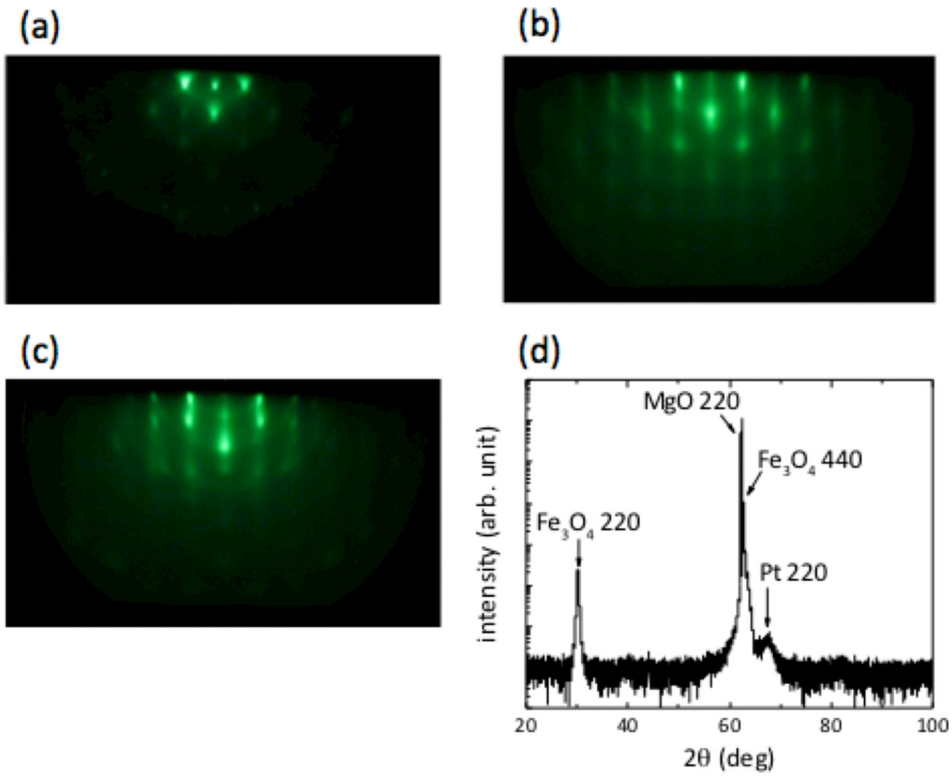

FIG. 1. *In situ* RHEED patterns of surfaces in the MgO(110)/NiO/Fe_3O_4/Pt/Fe layer : (a) Fe_3O_4, (b) Pt, and (c) Fe. (d) XRD pattern of the MgO(110)/Fe_3O_4/Pt/Fe layer at θ–2θ. The intensity was plotted using logarithms for ease of finding the peaks.

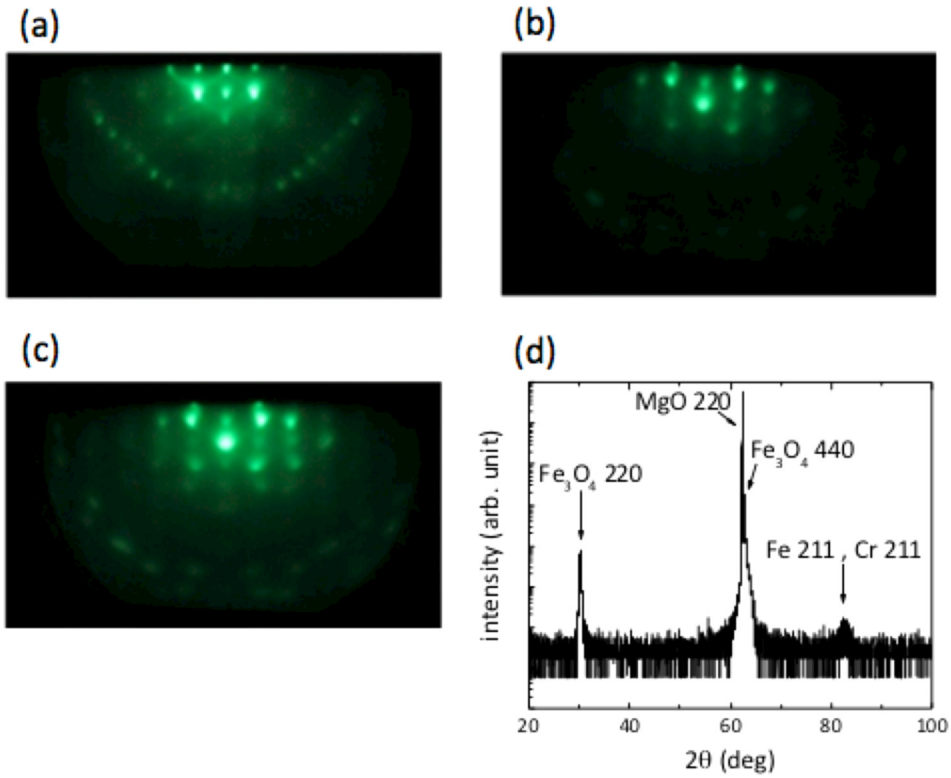

FIG. 2. *In situ* RHEED patterns of surfaces in the MgO(110)/NiO/Fe_3O_4/Cr/Fe layer: (a) Fe_3O_4, (b) Cr, and (c) Fe. (d) XRD pattern of the MgO(110)/Fe_3O_4/Cr/Fe layer at θ–2θ.

larger than that of bulk Fe because of the direct coupling between Fe_3O_4(110) and Fe. This coupling appeared to be ferromagnetic, as opposed to the Fe_3O_4(100)/Fe(100) antiferromagnetic coupling. Since the insertion of a thin nonmagnetic Pt layer ($t_{Pt} = 1.0$ nm) interrupted direct coupling, the H_c value decreased abruptly after the insertion of the layer. In addition, the shape of the hysteresis loop at t_{Pt} was different from that of the other loops, implying the existence of magnetic coupling. All hysteresis curves for the thicker Pt layers possess good squareness, and H_c is nearly constant. To investigate the properties of this relationship in greater detail, H_c was plotted as a function of t_{Pt} in Fig. 4(b). At a t_{Pt} of 0, the H_c value of Fe was enhanced significantly by direct magnetic coupling with Fe_3O_4(110). When $0 < t_{Pt} < 1.5$, the insertion of the Pt layer decreased the H_c value by a large degree, and H_c subsequently increased up to a t_{Pt} of 2.5 nm, after which H_c decreased and became constant. The behavior of this property seems to exhibit oscillation with damping.

Fig. 5(a) shows the hysteresis curves of the Fe_3O_4(110)/Cr/Fe system. At a t_{Cr} of 0, the H_c value exhibited a large field due to direct coupling and it decreased substantially with the insertion of the Cr layers, similar to that observed with Pt insertion. However, the behavior at t_{Cr} greater than 2 nm differed from that observed with Pt insertion: the H_c value of this system continued to increase up to a t_{Cr} of 10 nm. As shown in Fig. 5(b), H_c increased monotonically as a function of t_{Cr} and reached 400 Oe at a final t_{Cr} of 10 nm.

The H_c value of the two samples exhibited very different dependences on the NM layer thickness, with one showing an oscillatory behavior and the other a monotonic increase. In the sample with an inserted Pt layer, the oscillation is reminiscent of the IEC metallic systems. In their investigation of the IEC in Co/Pt multilayers, Knepper and Yang found that the H_c value of this system varied with the Pt thickness,[26] a behavior very similar to the variation in Fig. 4(b). Although the magnetic materials used in the two cases were different, the characteristics of the IEC remained dependent on the electronic properties of the nonmagnetic layer,[25] the Pt layer. Therefore, the IEC may be the origin of the observed variation of H_c with t_{Pt}.

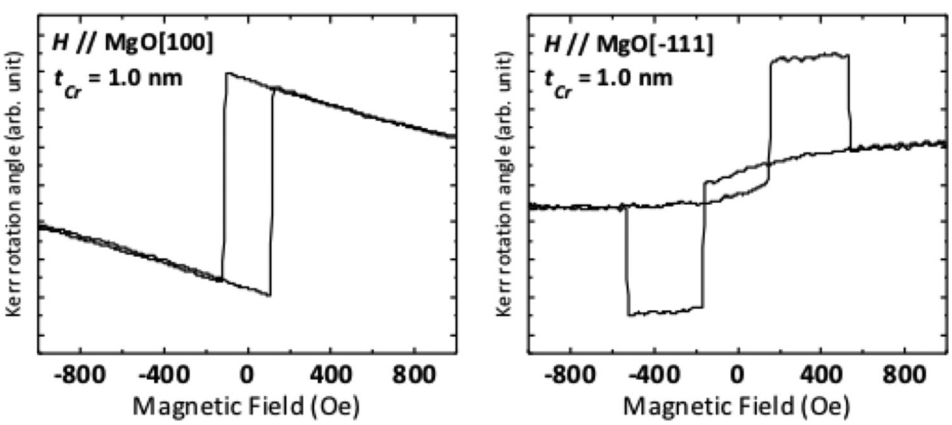

FIG. 3. Hysteresis loops of a MgO(110)/NiO(5 nm)/Fe_3O_4(60 nm)/Cr(1 nm)/Fe(5 nm) layer obtained by longitudinal MOKE measurement at RT when H was applied in the (a) MgO[−111] direction and (b) the MgO[100] direction.

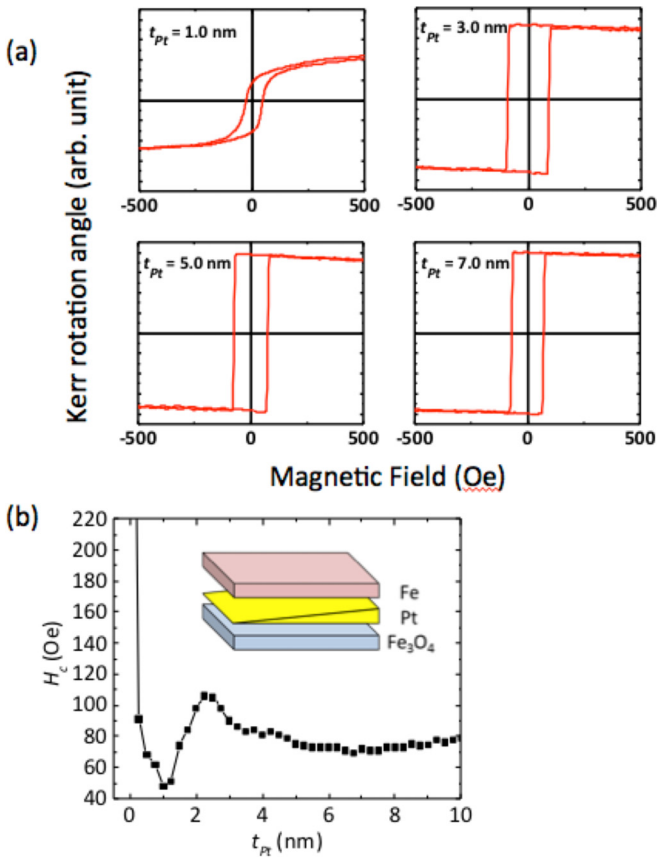

FIG. 4. (a) Hysteresis curves of a MgO(110)/NiO/Fe_3O_4/Pt(t_{Pt})/Fe layer with t_{Pt} = 1.0, 3.0, 5.0, and 7.0. (b) Plot of H_c versus t_{Pt}. The inset shows a schematic of the sample structure.

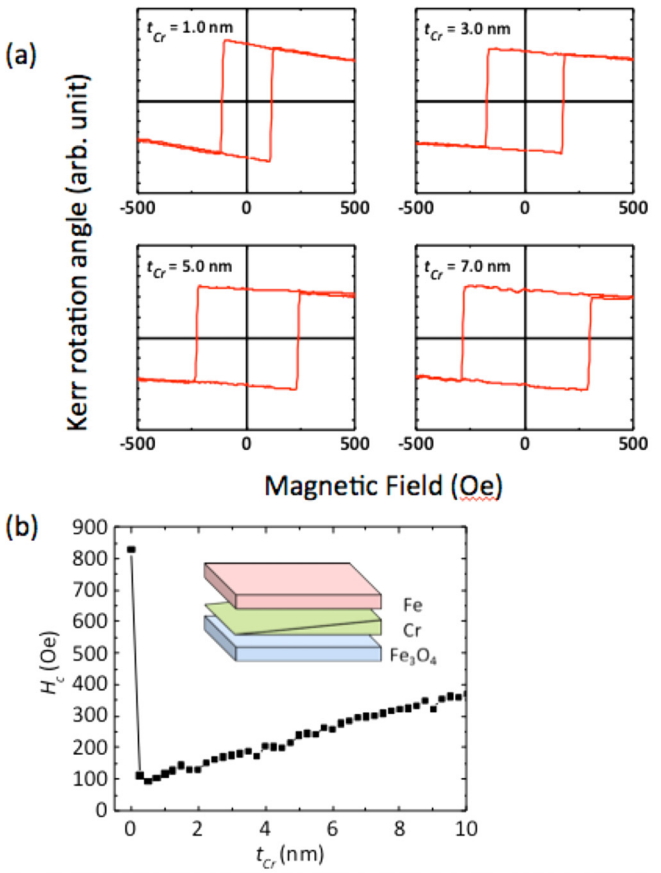

FIG. 5. (a) Hysteresis curves of a MgO(110)/NiO/Fe_3O_4/Cr(t_{Cr})/Fe layer with t_{Cr} = 1.0, 3.0, 5.0, and 7.0. (b) A plot of H_c versus t_{Cr}. The inset shows a schematic of the sample structure.

On the other hand, the sample with an inserted Cr layer showed puzzling behavior. The monotonic increase in H_c here is not characteristic of IEC. In a detailed investigation of the IEC for a Fe/Cr(211) multilayer grown on a MgO(110) substrate, Fullerton *et al.* observed a clear oscillation of the saturation fields,[30] which disagrees with the results of the present study. The lattice distortion is therefore the probable origin for the increase in H_c. In order to confirm this theory, a MgO(110)/Cr(t_{Cr})/Fe trilayer was fabricated and MOKE measurements were performed. Since the lattice parameters of MgO and Fe_3O_4 are almost identical, we expected the Cr lattice on MgO to distort in the same way as on Fe_3O_4(110). As shown in Fig. 6, the magnetization of the Fe layer switched in a small magnetic field, and the H_c value was almost independent of t_{Cr}. Therefore, the lattice distortion did not cause the increase in H_c. The interface effect (also known as the intermixing or proximity effect) was also unlikely to be the cause of the observed large H_c because H_c increased with increasing t_{Cr}. Furthermore, the interface effect is generally more applicable to thinner films. Thus, the cause of the increase in H_c remains unclear; further investigation using both experimental and theoretical approaches is necessary in order to understand this phenomenon.

We investigated the magnetization characteristics of Fe_3O_4(110)/[Pt (t_{Pt}) or Cr(t_{Cr})]/Fe systems of various thicknesses of the NM layer, and we found that H_c varied with t_{Pt}. In contrast, H_c increased drastically with the use of Cr insertion layers. The observed increase in H_c enables the control of the magnetic properties of the Fe layer in this hybrid

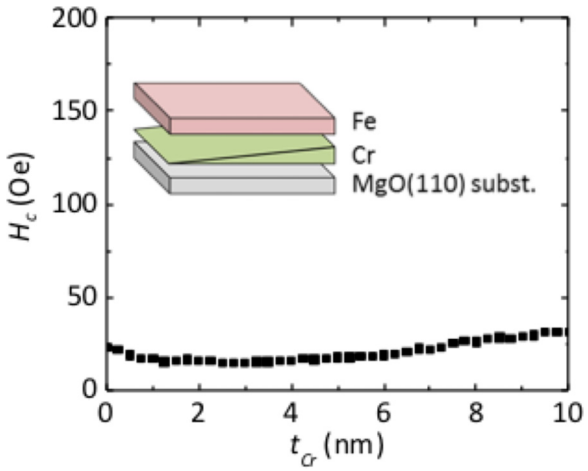

FIG. 6. Plot of H_c of the MgO(110)/Cr(t_{Cr})/Fe layer versus t_{Cr}. The inset shows a schematic of the sample structure.

system by varying the thickness of the Cr insertion layer. In order to understand the origin of this phenomenon, further experimental investigations on the multilayer's structure and theoretical calculations for this material are necessary.

This work was partly supported by JSPS KAKENHI under Grant Nos. 15H05702 and 23686006, the Collaborative Research Program of Institute for Chemical Research, Kyoto University (Grant No. 2016-57), and the OPEN FACILITY, Hokkaido University Sousei Hall.

[1]K. Uchida, J. Xiao, H. Adachi, J. Ohe, S. Takahashi, J. Ieda, T. Ota, Y. Kajiwara, H. Umezawa, H. Kawai, G. E. W. Bauer, S. Maekawa, and E. Saitoh, Nat. Mater. **9**, 894 (2010).
[2]E.-J. Guo, A. Herklotz, A. Kehlberger, J. Cramer, G. Jakob, and M. Kläui, Appl. Phys. Lett. **108**, 022403 (2016).
[3]M. Isasa, A. Bedoya-Pinto, S. Vélez, F. Golmar, F. Sánchez, L. E. Hueso, J. Fontcuberta, and F. Casanova, Appl. Phy. Lett. **105**, 142402 (2014).
[4]M. Opel, S. Geprägs, E. P. Menzel, A. Nielsen, D. Reisinger, K.-W. Nielsen, A. Brandlmaier, F. D. Czeschka, M. Althammer, M. Weiler, S. T. B. Goennenwein, J. Simon, M. Svete, W. Yu, S.-M. Hühne, W. Mader, and R. Gross, Phys. Status Solidi A **208**, 232–251 (2011).
[5]T. Nagahama, Y. Matsuda, K. Tate, T. Kawai, N. Takahashi, S. Hiratani, Y. Watanabe, T. Yanase, and T. Shimada, Appl. Phys. Lett. **105**, 102410 (2014).
[6]M. G. Chapline and S. X. Wang, Phys. Rev. B **74**, 014418 (2006).
[7]A. V. Ramos, M.-J. Guittet, J.-B. Moussy, R. Mattana, C. Deranlot, F. Petroff, and C. Gatel, Appl. Phys. Lett. **91**, 122107 (2007).
[8]Y. K. Takahashi, S. Kasai, T. Furubayashi, S. Mitani, K. Inomata, and K. Hono, Appl. Phys. Lett. **96**, 072512 (2010).
[9]G. S. Parkinson, Surf. Sci. Rep. **71**, 272–365 (2016).
[10]W. B. Mi, J. J. Shen, E. Y. Jiang, and H. L. Bai, Acta Mater. **55**, 1919–1926 (2007).
[11]E. J. Verwey, Nature **144**, 327 (1939).
[12]W. Mi, Z. Guo, Q. Wang, Y. Yang, and H. Bai, Scr. Mater. **68**, 972–975 (2013).
[13]M. S. Senn, J. P. Wright, and J. P. Attfield, Nature **481**, 173–176 (2012).
[14]X. Liu, L. Yin, and W. Mi, Sci. Rep. **7**, 43403 (2017).
[15]A. Yanase and K. Siratori, J. Phys. Soc. Jpn. **53**, 312 (1984).
[16]S. Yuasa, T. Nagahama, A. Fukushima, Y. Suzuki, and K. Ando, Nat. Mater. **3**, 868 (2004).
[17]S. S. P. Parkin, C. Kaiser, A. Panchula, P. M. Rice, B. Hughes, M. Samant, and S. H. Yang, Nat. Mater. **3**, 862 (2004).
[18]M. Bibes and A. Barthélémy, IEEE Trans. Electron Devices **54**, 1003 (2007).
[19]J. Noguésa and I. K. Schuller, J. Magn. Magn. Mater. **192**, 203 (1999).
[20]S. S. P. Parkin, N. More, and K. P. Roche, Phys. Rev. Lett. **64**, 2304 (1990).
[21]H. Yanagihara, Y. Toyoda, A. Ohnishi, and E. Kita, Appl. Phys. Exp. **1**, 111303 (2008).
[22]H. Yanagihara, Y. Toyoda, and E. Kita, J. Phys. D.: Appl. Phys. **44**, 064011 (2011).
[23]P. A. A. van der Heijden, P. J. H. Bloemen, J. M. Metselaar, R. M. Wolf, J. M. Gaines, J. T. W. M. van Eemeren, P. J. van der Zaag, and W. J. M. de Jonge, Phys. Rev. B **55**, 11569 (1997).
[24]H.-C. Wu, S. K. Arora, O. N. Mryasov, and I. V. Shvets, Appl. Phys. Lett. **92**, 182502 (2008).
[25]M. D. Stiles, J. Magn. Magn. Mater. **200**, 322 (1999).
[26]J. W. Knepper and F. Y. Yang, Phys. Rev. B. **71**, 224403 (2005).
[27]Y. Gao, Y. J. Kim, S. A. Chambers, and G. Bai, J. Vac. Sci. Technol. A **15**, 332 (1997).
[28]K. A. Shaw, E. Lochner, and D. M. Lind, J. Appl. Phys. **87**, 1727 (2000).
[29]C. Gatel, E. Snoeck, V. Serin, and A. R. Fert, Eur. Phys. J. B **45**, 157–168 (2005).
[30]E. E. Fullerton, M. J. Conover, J. E. Mattson, C. H. Sowers, and S. D. Bader, Phys. Rev. B. **48**, 21 (1993).
[31]K. Shikada, K. Tabuchi, M. Ohtake, F. Kirino, and M. Futamoto, J. Magn. Soc. Jpn. **32**, 296 (2008).